Activation of *Big Grain1* significantly improves grain size by regulating auxin transport in rice

Linchuan Liu[1], Hongning Tong[1], Yunhua Xiao, Ronghui Che, Fan Xu, Bin Hu, Chengzhen Liang, Jinfang Chu, Jiayang Li[2], and Chengcai Chu[2]

State Key Laboratory of Plant Genomics and National Center for Plant Gene Research (Beijing), Institute of Genetics and Developmental Biology, Chinese Academy of Sciences, Beijing 100101, China

Contributed by Jiayang Li, June 30, 2015 (sent for review January 12, 2015; reviewed by Hongxuan Lin, Makoto Matsuoka, and Yunde Zhao)

Grain size is one of the key factors determining grain yield. However, it remains largely unknown how grain size is regulated by developmental signals. Here, we report the identification and characterization of a dominant mutant *big grain1* (*Bg1-D*) that shows an extra-large grain phenotype from our rice T-DNA insertion population. Overexpression of *BG1* leads to significantly increased grain size, and the severe lines exhibit obviously perturbed gravitropism. In addition, the mutant has increased sensitivities to both auxin and N-1-naphthylphthalamic acid, an auxin transport inhibitor, whereas knockdown of *BG1* results in decreased sensitivities and smaller grains. Moreover, *BG1* is specifically induced by auxin treatment, preferentially expresses in the vascular tissue of culms and young panicles, and encodes a novel membrane-localized protein, strongly suggesting its role in regulating auxin transport. Consistent with this finding, the mutant has increased auxin basipetal transport and altered auxin distribution, whereas the knockdown plants have decreased auxin transport. Manipulation of *BG1* in both rice and *Arabidopsis* can enhance plant biomass, seed weight, and yield. Taking these data together, we identify a novel positive regulator of auxin response and transport in a crop plant and demonstrate its role in regulating grain size, thus illuminating a new strategy to improve plant productivity.

grain size | *Big Grain1* | auxin | biomass | grain yield

Because it is one of the most important staple food crops cultivated worldwide, improvement of grain yield is a major focus of rice-breeding programs (1). Grain size is one of the determining factors of grain yield (2, 3). A number of quantitative trait loci (QTLs) controlling rice grain size have been identified in recent years (4–11). However, functional mechanisms of these genes remain largely unknown. Because QTLs usually have important functions in determining grain size, many of them have been widely selected in breeding processes or existed in modern elite varieties, and a certain QTL could be only applicable in certain varieties (12). Thus, exploration of new grain size-associated genes and elucidation of their functional mechanisms have great significance for further improvement of rice yield (12).

Seed size, as well as other organ size, is controlled by various plant hormones, such as auxin, brassinosteroid, and cytokinin (10, 13, 14). A number of studies have demonstrated that auxin plays a vital role in organ size determination by affecting cell division, cell expansion, and differentiation (15–17). Auxin exists predominantly as indole-3-acetic acid (IAA) in plants, and genetic studies of its biosynthetic genes in *Arabidopsis* have demonstrated that IAA regulates many aspects of plant growth and development, including stem elongation, lateral branching, vascular development, and tropic growth responses (18, 19). Combined with biochemical studies, the tryptophan (Trp)-dependent IAA biosynthesis pathway has been clearly established involving the YUCCA family flavin monooxgenases (20). Importantly, the two-step pathway is highly conserved throughout the plant kingdom (21). Until very recently, the Trp-independent auxin biosynthetic pathway was elucidated as contributing to early embryogenesis in *Arabidopsis* (22). Primary auxin signaling is a rapid process initiated from the hormone perception by receptor TIR1, an F-box protein, followed by degradation of the negative regulator AUX/IAA proteins, and further release the downstream auxin response factors (ARFs) (23–26). However, how the ARFs work in plants remains elusive. Auxin transport, generally referring to the cell-to-cell transportation of the hormone directed basipetally from shoots to roots in vascular tissues, plays a critical role in auxin response (18). The transport involves a number of membrane-associated proteins, such as PINs (protein inhibitor of nNOS), AUX1 (AUXIN TRANSPORTER PROTEIN 1), and ABCBs (ATP-BINDING CASSETTE, SUB-FAMILY B PROTEINS) as efflux or influx carriers (27–30). Disruption of auxin transport induced by either gene mutations or chemical inhibitor treatment will lead to diverse development defects, such as decreased lateral organ initiation and defective tropic growth responses (27, 31–34).

In this study, we identify a rice mutant, named *big grain1-D* (*Bg1-D*) because it is a dominant mutant having extralarge grain size. *BG1* encodes a novel plasma membrane-associated protein, and is specifically induced by auxin treatment. We show that BG1 is a new positive regulator of auxin response involved in auxin transport, and demonstrate that manipulation of *BG1* expression can greatly improve grain size and plant productivity.

Results

***Bg1-D* Shows Increased Grain Size Phenotype.** We have identified a number of rice mutants with altered grain size from our T-DNA

Significance

As one of the most important growth-promoting hormones, auxin regulates many aspects of plant growth and development. Understanding auxin action has long been a challenging task because of the complexity of the hormone transport involved in auxin response. Despite tremendous progress made in *Arabidopsis*, auxin response and transport are poorly understood in crop plants, which impedes the application of hormone knowledge in agricultural improvement. This study not only identifies a novel positive regulator of plant growth in rice and demonstrates its significant role in improving seed size and grain yield, it also illustrates the specific involvement of the plasma membrane-associated protein in regulating auxin response and transport, thus illuminating a new strategy for enhancing crop productivity.

Author contributions: L.L., H.T., J.L., and C.C. designed research; L.L., H.T., Y.X., R.C., F.X., B.H., C.L., and J.C. performed research; L.L., H.T., J.L., and C.C. analyzed data; L.L., H.T., J.L., and C.C. wrote the paper; and J.L. and C.C. supervised the project.

Reviewers: H.L., Institute of Plant Physiology and Ecology, Chines Academy of Sciences; M.M., Nagoya University; and Y.Z., University of California, San Diego.

The authors declare no conflict of interest.

Freely available online through the PNAS open access option.

[1]L.L. and H.T. contributed equally to this work.

[2]To whom correspondence may be addressed. Email: jyli@genetics.ac.cn or ccchu@genetics.ac.cn.

This article contains supporting information online at www.pnas.org/lookup/suppl/doi:10.1073/pnas.1512748112/-/DCSupplemental.

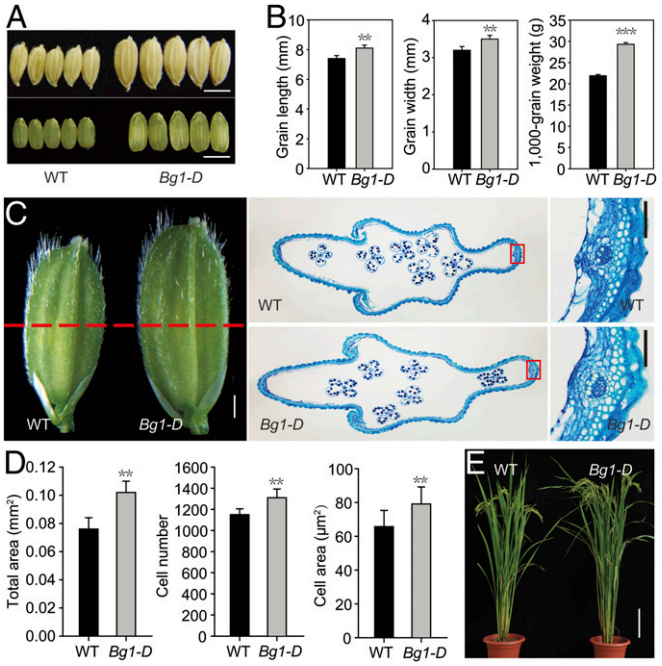

Fig. 1. Phenotype of *Bg1-D* mutant. (*A*) Grain morphology of WT and *Bg1-D*. (Scale bar, 0.5 cm.) (*B*) Statistical data of the grain length, grain width, and 1,000-grain weight in WT and *Bg1-D*. (*C*) Cross-sections of the spikelet hulls of WT and *Bg1-D*. Dashed line indicates the position of the cross-section. (Scale bar, 1 mm.) Magnified views in the boxes are shown. (Scale bar, 0.1 mm.) (*D*) Statistical data of the total area, cell number and cell area in the outer parenchyma layer of the spikelet hulls of WT and *Bg1-D*. (*E*) Gross morphology of 4-mo-old plants of WT and *Bg1-D* grown in paddy field. (Scale bar, 20 cm.) Means ± SD are given in *B* ($n = 20$) and *D* ($n = 15$). $^{**}P < 0.01$. $^{***}P < 0.001$ (*t* test).

insertion population. Among them, *Bg1-D* has the most obviously increased grain size (Fig. 1*A*). Compared with WT (Nipponbare, *Oryza sativa* L. ssp. *japonica*), the 1,000-grain weight of *Bg1-D* has increased about 33.8%, with the grain length and grain width increased about 15.2% and 17.0%, respectively (Fig. 1*B*). Observation of spikelet hull by scanning electron microscopy showed that the epidermis cells of both palea and lemma in *Bg1-D* are much longer than that of the WT (Fig. S1). Careful examination of the hull cross-section before flowering revealed significant increases of both number and area of the parenchyma cells in the *Bg1-D* mutant (Fig. 1 *C* and *D*). Consistent with this, a number of genes associated with cell cycle and cell expansion were up-regulated in the panicles of the *Bg1-D* mutant (Fig. S2).

Despite the greatly enlarged grain size, *Bg1-D* also exhibits enhanced growth of other tissues at both the vegetative and reproductive stages (Fig. 1*E* and Fig. S3). One-week-old seedlings of the *Bg1-D* mutant have obviously increased length of leaf and root compared with WT (Fig. S3 *A*–*D*). When plants enter reproductive stage, the leaves of *Bg1-D* are longer and wider than those of the WT plants, and the *Bg1-D* also has increased plant height (Fig. 1*E*, Fig. S3*E*, and Table S1). In addition, the *Bg1-D* panicles are much larger than those of the WT (Fig. S3 *F* and *G*).

We also compared the fresh and dry weights of seeds between the *Bg1-D* and WT, and found that the weight of *Bg1-D* endosperms was markedly increased compared with that of WT at 15 days after fertilization, and the difference reached a maximum at 25 days after fertilization (Fig. S4). Thus, the significant overall improvement of the grain weight in the *Bg1-D* mutant is attributed to the increases in both hull size and endosperm volume.

Molecular Cloning of *BG1*. Genetic analyses showed that F_1 progenies of the reciprocal crosses between *Bg1-D* and WT have big grain phenotype (Fig. S5*A*). In addition, the phenotype of *Bg1-D* cosegregates with the T-DNA insertion in the F_2 population, and the segregation ratio is ∼3:1 (Fig. S5*B*), suggesting that the mutant phenotype is caused by a T-DNA insertion, which activates the expression of *BG1*. We cloned the T-DNA 3′-flanking sequence by the site-finding PCR method based on thermal asymmetric interlaced PCR (35, 36). Sequence analysis revealed that a T-DNA was inserted at 0.8 kb upstream of the gene *Os03g0175800* (Fig. 2*A*). Additional gene-expression analysis showed that, whereas other adjacent genes of the insertion site have comparable transcript levels in the mutant and WT, this gene has increased expression ∼10-fold in the *Bg1-D* mutant (Fig. 2*B*). Thus, *Os03g0175800* is potentially the gene responsible for the *Bg1-D* mutant phenotypes and was designated as *BG1*.

BG1 Is a Novel Positive Regulator That Controls Grain Size. The full-length cDNA of *BG1* was amplified by 5′ RACE, which is 1,190 bp in length and contains an ORF of 933 bp encoding 330 amino acids. To verify that activation of *BG1* is responsible for the mutant phenotype, we overexpressed *BG1* cDNA under the control of the rice *ACTIN1* promoter in WT and found that the *BG1*-overexpressing plants (*BG1-OE*) showed obviously increased grain size and other phenotypes, such as enhanced plant height, longer leaves, and larger panicles, which resemble the *Bg1-D* mutant phenotypes (Fig. 2*C* and Fig. S6 *A* and *B*). Importantly, severity of the phenotypes was apparently correlated with the *BG1* expression level; that is, plants with higher *BG1* expression have bigger grain size as well as increased 1,000-grain weight (Fig. 2 *D*–*G*), demonstrating that activation of *BG1* is the cause for the *Bg1-D* mutant phenotypes.

Suppression of *BG1* by RNA interference (*BG1-Ri*) led to obviously opposite phenotypes, including reduced plant height and decreased panicle length and grain size, as well as reduced 1,000-grain weight (Fig. 2 *H*–*K* and Fig. S6 *C* and *D*). The phenotype severity is

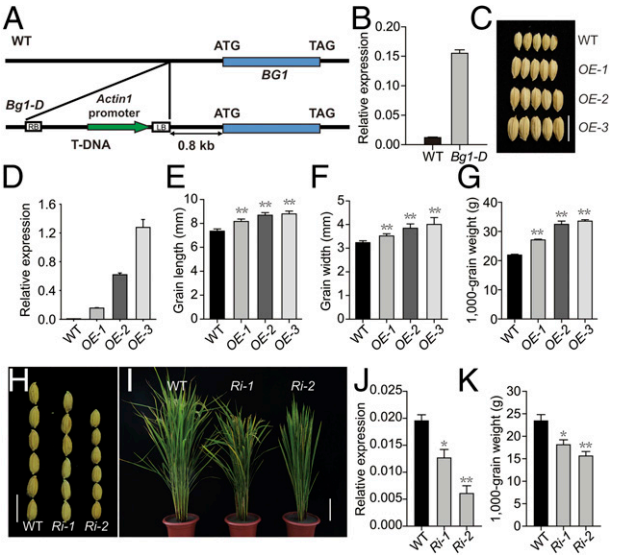

Fig. 2. Cloning of *BG1* gene and verification of BG1 function. (*A*) Schematic map of the T-DNA flanking region in *Bg1-D* mutant. The T-DNA contains rice *ACTIN1* promoter near the left border (LB), which is 0.8 kb upstream of *BG1* (*Os03g0175800*). (*B*) The expression level of *BG1* in WT and *Bg1-D*. (*C*) Grain morphology of WT and *BG1*-overexpressing plants (*OEs*). (Scale bar, 1 cm.) (*D*) Expression level of *BG1* in WT and *OEs*. (*E*–*G*) Statistical data of the grain length (*E*), grain width (*F*), and 1,000-grain weight (*G*) in WT and *OEs*. (*H*) Grain morphology. (Scale bar, 1 cm.) (*I*) Gross plant morphology. (Scale bar, 20 cm.) (*J*) *BG1* expression level. (*K*) 1,000-grain weight in WT and *BG1*-knockdown plants (*Ris*). Means ± SD are given in *E* and *F* ($n = 20$) and *G* and *K* ($n = 5$) $^{*}P < 0.05$, $^{**}P < 0.01$ (*t* test).

also consistent with the *BG1* expression level, suggesting that the native *BG1* indeed controls grain size and plant growth in rice.

Molecular Characterization of BG1. BLAST search of the protein databases discovered a number of orthologous proteins of BG1 in various higher plants. Phylogenetic analysis showed that the proteins can be classified into two subgroups: dicot- and monocot-specific groups (Fig. S7). However, none of them has been functionally characterized, including four *Arabidopsis* BG1-like proteins. Moreover, no known functional domain in these proteins could be found, suggesting that BG1 is a novel plant-specific regulator controlling organ size.

Quantitative RT-PCR analysis showed that *BG1* transcripts can be detected in various tissues, but the expression is relatively stronger in culms and panicles, and the level is gradually decreased as the panicle matures (Fig. 3*A*). We also analyzed the *BG1* promoter activity in various tissues of PRO_{BG1}*:GUS* transgenic plants. GUS staining revealed that the *BG1* promoter is specifically active in the vascular tissues of leaves, culms, and hulls (Fig. 3*B*). Furthermore, RNA in situ hybridization of developing hulls demonstrated the preferential expression of *BG1* in hull vascular tissues with a gradual decrease as the development progressed (Fig. 3*B* and Fig. S8*E*).

BG1 Is Localized to the Plasma Membrane. Because *BG1* encodes a novel protein without known sequence characteristics, we first investigated the protein subcellular localization. A *35S:BG1-eGFP* vector containing eGFP-tagged BG1 was introduced into WT rice, and transgenic plants displayed obvious phenotypes similar to the *Bg1-D* mutant (Fig. S8 *A*–*C*), indicating that the fused BG1-eGFP is functional. GFP fluorescence observation using roots as material showed that the protein is predominantly localized to the plasma membrane (Fig. 3*C*). Consistent with this finding, we also obtained a similar result in rice protoplasts transformed with the same vector (Fig. S8*D*). To confirm these results, we separated the microsomes of the transgenic plants and then detected the proteins by anti-GFP antibodies. Immunoblotting results showed that BG1-eGFP can be obviously detected in the microsomal pellets, but only a very faint signal was observed in the soluble fraction (Fig. 3*D*). An additional two-phase partitioning assay demonstrated that the BG1-eGFP protein was highly enriched in the plasma membrane fraction, but not in the other membrane's fractions (Fig. 3*E*).

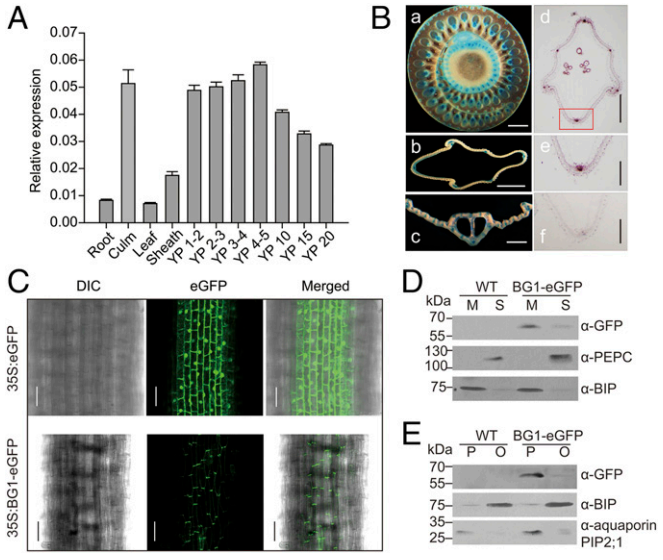

Fig. 3. *BG1* expression pattern and protein subcellular localization. (*A*) Expression of *BG1* in various organs analyzed by quantitative analysis. Root, culm, leaf, and leaf sheath were harvested from 2-mo-old WT plants. Young panicles (YP) in different lengths (indicated as numbers, cm) were included for the analysis. (*B*) GUS staining of various tissues of PRO_{BG1}*:GUS* transgenic plants and RNA in situ hybridization. (*a*) Cross-section of young culm. (Scale bar, 1 mm.) (*b*) Cross-section of hull. (Scale bar, 500 μm.) (*c*) Cross-section of leaf. (Scale bar, 1 mm.) (*d*) In situ localization of *BG1* mRNA in the hull from 5-cm length young panicle. (Scale bar, 500 μm.) (*e*) Magnified views of the boxed area in *d*. (Scale bar, 200 μm.) (*f*) Negative control. (Scale bar, 200 μm.) (*C*) Confocal observation of root of the transgenic plants with *35S:eGFP* (*Upper*) and *35S:BG1-eGFP* (*Lower*). (Scale bar, 50 μm.) DIC indicates the differential interference contrast phase. (*D*) Microsomes separation and detection of BG1 by anti-GFP antibody. M, microsomes; S, soluble fraction. Blotting signals with anti-PEPC and anti-BIP were used as controls. (*E*) Further plasma membrane isolation and detection of BG1 by anti-GFP antibody. P, plasma membrane fraction; O, other fractions. Blotting signals with anti-BIP and antiaquaporin PIP2;1 were used as controls.

***BG1* Is a Primary Auxin Response Gene.** To investigate whether phytohormones affect *BG1* transcription, we analyzed *BG1* expression in WT seedlings under the treatment of various hormones. After 2-h application of hormones, we found that *BG1* is specifically induced by IAA, but not by others (Fig. 4*A*). An additional time-course analysis revealed that the *BG1* transcript level was rapidly induced within 30 min of IAA application and the expression reached the maximum with ∼eightfold of that without hormone treatment after 4-h treatment (Fig. 4*B*). The IAA-induced accumulation still occurred in the presence of cycloheximide (CHX), a protein synthesis inhibitor, suggesting that the induction does not rely on protein synthesis (Fig. 4*C*). Moreover, IBA (indole-3-butyric acid) and NAA (naphthylacetic acid) (two other auxin compounds) can also induce the expression of *BG1*, but to a less extent, whereas tryptophan (a structurally similar molecule to IAA) failed to induce *BG1* accumulation (Fig. 4*D*), showing no hormonal activity. These results strongly suggest that *BG1* is a novel specific and primary auxin response gene. Consistent with this, we found that *Bg1-D* had increased sensitivity to IAA in term of root elongation/inhibition and, in contrast, *BG1-Ri* plants had greatly decreased sensitivity to IAA (Fig. 4*E* and Fig. S9*A*), demonstrating that BG1 is involved in auxin response.

***BG1* Is Involved in Auxin Transport.** In *BG1*-overexpression plants, a number of lines with high expression levels of *BG1* showed obviously enlarged tiller angles (Fig. 4 *F* and *G*), a phenotype associated with perturbed auxin transport (33). Combined with the membrane localization of the BG1 protein and the induction of *BG1* by auxin treatment, these results strongly imply that BG1 is involved in auxin transport. Strikingly, we further observed that these *BG1*-overexpressing lines have obvious defects in tropic growth at the young seedling stage. When their seeds were sowed on agar culture media, with a high frequency, both the roots and the shoots grew in a slanting direction, and in some cases the roots even grew upward, resembling the NPA (N-1-naphthylphthalamic acid, an auxin transport inhibitor)-treated phenotype (Fig. 4*H* and Fig. S9*B*). To test whether the *Bg1-D* mutant also has altered gravitropism response, we treated the *Bg1-D* mutant, WT, and *BG1-Ri* plants with 0.1 μM NPA and then compared their phenotypes (Fig. 4*I* and Fig. S9*C*). In plant shoots, whereas a few of the WT plants had slightly oblique growth under low concentration of NPA, *BG1-Ri* plants had normal growth. In contrast, ∼35% of *Bg1-D* mutant shoots grew downward into the culture medium. In roots, NPA strongly inhibited the lateral root initiation in all of the three plants. However, compared with those without treatment, the root tip numbers of WT, *Bg1-D*, and *BG1-Ri* plants were repressed to 21.8%, 17.7%, and 37.3%, respectively (Fig. 4*J*), indicating that the NPA effect is more remarkable on *Bg1-D* but less on *BG1-Ri* than on WT. In conclusion, *Bg1-D* has increased sensitivity to NPA, whereas *BG1-Ri*

PLANT BIOLOGY

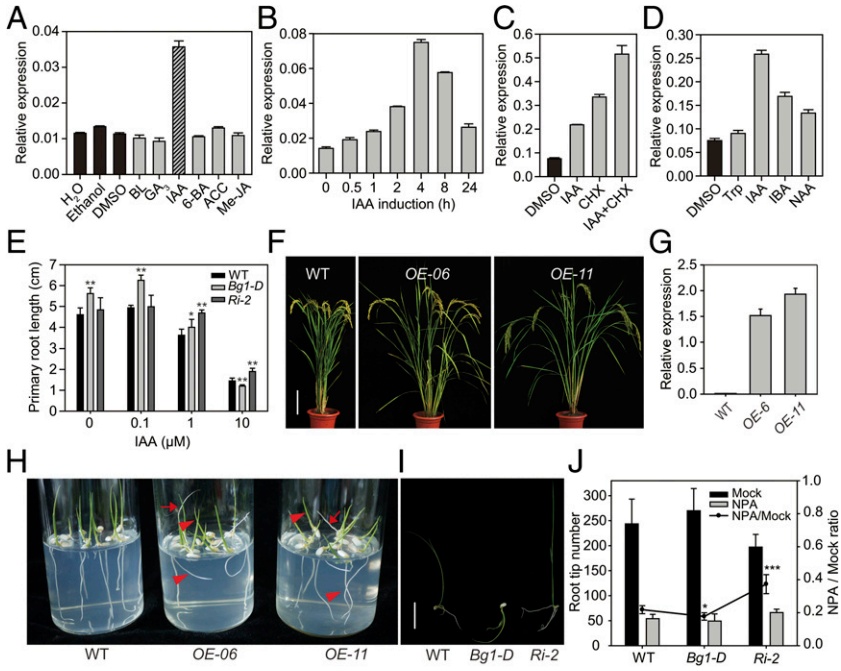

Fig. 4. *BG1* is a specific auxin response gene. (*A*) Relative expression level of *BG1* under different phytohormone treatments. BL, brassinolide; GA_3, gibberellic acid; IAA, indole-3-acetic acid; 6-BA, 6-benzylaminopurine; ACC, 1-aminocyclo-propane-1-carboxylic acid; JA, jasmonic acid. (*B*) Time-course response of *BG1* to 10 μM IAA treatment. (*C*) Effect of CHX on *BG1* expression. (*D*) *BG1* response to different auxin compounds. (*E*) Effects of different IAA concentrations on primary root length in WT, *Bg1-D*, and *Ri-2*. (*F*) Gross morphology of WT and two independent *BG1*-overexpression lines (*OEs*) at the reproductive stage. (Scale bar, 20 cm.) (*G*) *BG1* expression levels in the plants shown in *F*. (*H*) Growth of the plants on agar medium. Arrows indicate the upward growth of roots. Arrowheads indicate slanting growth of shoots and roots. (*I*) Growth of WT, *Bg1-D*, and *Ri-2* under 0.1 μM NPA treatment. (Scale bar, 1 cm.) (*J*) Statistical data of root tip number of WT, *Bg1-D*, and *Ri-2* under 0.1 μM NPA treatment. Means ± SD are given in *E* ($n = 20$) and *J* ($n = 10$). $^*P < 0.05$, $^{**}P < 0.01$, $^{***}P < 0.001$ (*t* test). Zhonghua 11 was used as WT in *F*–*H*.

has decreased sensitivity. Taken together, these results strongly suggest that BG1 is involved in auxin transport.

***Bg1-D* Exhibits Altered IAA Distribution and Transport.** *DR5:GUS* has been widely used as a reporter to study endogenous auxin distribution (37). To study whether activation of *BG1* caused altered auxin distribution, we crossed the *DR5:GUS* plants to *Bg1-D*, and then analyzed the *DR5* promoter activity in the double mutant by GUS staining. Compared with the *DR5:GUS* plants where the GUS signal was mainly detected at the apex area in both roots and spikelets, the GUS expression in the *Bg1-D* mutant was more intense and covered a much broader area, indicating that the *Bg1-D* mutant had enhanced auxin distribution in these tissues (Fig. 5 *A* and *B*). Consistent with this finding, the IAA level was markedly increased in the panicles of the *Bg1-D* mutant compared with WT (Fig. 5*C*). In addition, we directly measured the basipetal IAA transport in the coleoptiles of dark-grown seedlings of WT, *Bg1-D*, and *BG1-Ri* plants. Compared with the WT, the *Bg1-D* mutant had an ∼50% increase in the basipetal IAA transport, whereas *BG1-Ri* had decreased transport (Fig. 5*D*), further confirming that BG1 is involved in auxin transport.

Manipulation of *BG1* Increases Plant Biomass and Grain Yield. Because activation of *BG1* leads to a marked increase in grain size and grain weight, we tested whether *BG1* can be applied to improve grain yield. We found that most of the *BG1*-overexpressing plants, including the *Bg1-D* mutant, have insignificant change of grain yield per plant because of a lower percentage of full matured grains compared with the WT plants, which may be caused by ectopic expression of *BG1* under a strong constitutive promoter. To deal with this problem, we introduced the *BG1* gene into WT plants using a 3.6-kb genomic fragment containing the 2-kb native promoter and the entire coding region of *BG1*, as well as a 667 bp downstream sequence. Consistent with the predominant role of BG1 in panicle development, the transgenic plants showed obviously increased grain size and larger panicle without other obviously negative effects (Fig. 6 *A*–*C*). Statistical analysis showed that the 1,000-grain weight of two lines, *OE-5* and *OE-7*, increased 15.48% and 25.38%, respectively, and the grain yield per plant increased 6.69% and 16.65%, respectively, compared with WT (Fig. 6 *D* and *E*). An additional field trial test showed that the actual yield per plot (15 m^2) of both transgenic lines had increased about 15.1% and 20.8%, respectively (Table S2).

Despite the increased grain weight, overexpression of *BG1* also significantly enhanced plant biomass, with the highest about 18% increase of dry weight in three analyzed lines (Fig. S10*A*). In contrast, the *BG1-Ri* lines showed greatly decreased biomass. In addition, we also generated a *35S:BG1* vector and introduced it into *Arabidopsis* (Columbia, Col-0), and found that overexpression of *BG1* in *Arabidopsis* also resulted in greatly increased seed size and enhanced growth at both vegetative (Fig. S10 *B* and *C*) and reproductive (Fig. 6 *F* and *G*) stages, suggesting that *BG1* is also functional in dicots. Considering that orthologs of BG1 exist in many other plant species, including sorghum, Medicago, maize, and soybean (Fig. S7), BG1 may have extensively practical roles in improving plant biomass and grain productivity in various species.

Discussion

Several lines of evidence support the involvement of BG1 in auxin transport. First, BG1 is localized to plasma membrane, expresses in vascular tissues, and is induced by auxin treatment. These characteristics are reminiscent of typical auxin transport genes, such as *PINs* (28, 38). Second, *Bg1-D* has increased sensitivities to both auxin and NPA, whereas *BG1-Ri* has decreased sensitivities. Severe *BG1*-overexpressing lines have obviously

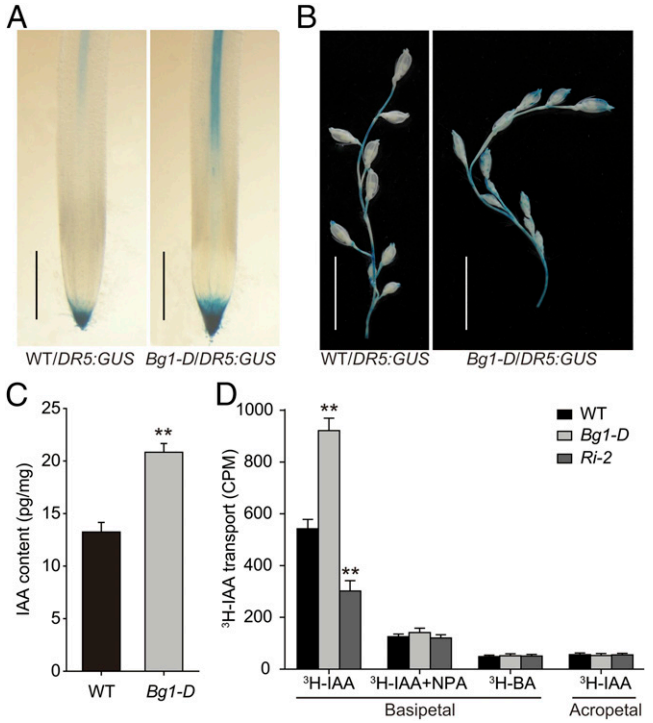

Fig. 5. Altered auxin distribution and transport in *Bg1-D* mutant. (*A* and *B*) Comparison of *DR5* promoter activity in root (*A*) and spikelet (*B*) of WT and *Bg1-D* by GUS staining. (Scale bar, 1 mm in *A* and 1 cm in *B*). (*C*) Quantification of IAA content in panicles of WT and *Bg1-D*. (*D*) Measurement of auxin transport ability in WT, *Bg1-D*, and *Ri-2* using coleoptile as materials. Means ± SD are given in *C* ($n = 3$) and *D* ($n = 15$). $^{**}P < 0.01$ (*t* test).

defective gravitropism growth. Third, *Bg1-D* has obviously enhanced basipetal auxin transport, whereas *BG1-Ri* has decreased auxin transport. Therefore, it is very likely that BG1 plays an important role in controlling plant growth and development through regulating auxin transport. In *Arabidopsis*, auxin transport regulates a number of processes associated with cell expansion or division, including hypocotyl elongation, shade avoidance, and stamen filament elongation (39–42). In rice, overexpression of a small auxin-up RNA (*SAUR*) gene *SAUR39* reduces auxin transport, resulting in abnormal shoot and root growth and altered shoot morphology compared with WT plants (43). In addition, mutation of the *NARROW LEAF1* (*NAL1*) gene reduces polar auxin transport activity, leading to reduction in leaf size and stem length (44). Recently, *NAL1* has been identified as an important QTL regulating grain yield by three independent studies (45–47). Near-isogenic lines carrying a gain-of-function allele of *NAL1*, as well as the gene overexpressors, have increased leaf length, panicle size, and grain productivity. Importantly, this allele has been selected in high-yield rice-breeding process. Although the detailed mechanism of NAL1 function remains unclear, these results suggest a potential of modulating auxin transport in improving grain yield. Our study provides direct evidence that strengthened auxin transport caused by activation of *BG1* leads to enhanced growth, whereas suppression of *BG1* weakens auxin transport, resulting in reduced growth. Interestingly, although *Bg1-D* exhibits an overall enhanced growth in different tissues, the most significant change is the increased grain size and grain weight. Because grain weight depends to a large extent on the hull development and endosperm maturation, the role of auxin transport in coordination of this process needs to be further investigated.

So far, the detailed relationship between auxin transport and auxin signaling remains unclear. It appears that auxin transport determines its distribution, where auxin exerts its function through auxin signaling. However, abundant studies have demonstrated that a regional gradient of hormone concentrations, resulted by polar auxin transport and local auxin biosynthesis, is important for auxin-mediated developmental processes (48, 49). Consistent with this idea, *BG1-Ri* plants have obviously decreased IAA sensitivity. In addition, transcripts of both *BG1* and *PINs* are greatly induced by auxin treatment, and it has been shown that *PINs* up-regulation is dependent on AUX/IAA-mediated signaling pathway (38). We also found there are two auxin response elements in the *BG1* promoter, implying that *BG1* might be regulated by ARF. Thus, the auxin transport and auxin signaling may form a regulatory loop to stimulate each other, leading to a rapid and efficient auxin response (50, 51).

Because BG1 has no obvious membrane localization peptide sequence and hydrophobic regions, it seems unlikely that BG1 directly transports auxin. BG1 may interact with other membrane-localized auxin transporters, such as members of PIN, AUX1/LAX, or ABCB families (28, 29, 49), to modulate their activities or to facilitate the auxin transport. Several factors involved in vesicular trafficking or phosphorylation modification were reported to regulate PIN function (52, 53). A BIG protein has also been found to modulate PIN localization (54). Interestingly, whereas both BG1 and PIN appear to be involved in auxin transport, it is unexpected that some *BG1*-overexpressing plants have a similar phenotype as *OsPIN1*-knockdown plants, which also have enlarged tiller angles as well as enhanced NPA sensitivity (55). One possibility is that BG1 functions in a way different from PINs to regulate auxin transport. Mutation of *LAZY1* also leads to enlarged tiller angles with enhanced basipetal auxin transport (33). Further investigation on the relationship between BG1 and these transport-associated components is essential to elucidate the BG1 functional mechanism.

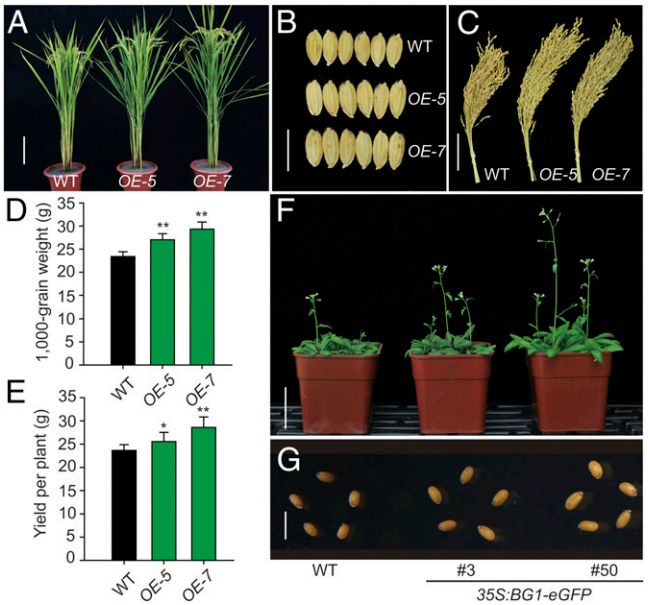

Fig. 6. Manipulation of *BG1* improves plant yield. (*A*) Gross morphology of WT and two independent genomic *BG1* transgenic plants, *OE-5* and *OE-7*. (Scale bar, 20 cm.) (*B*) Grain morphology of WT and the transgenic plants. (Scale bar, 1 cm.) (*C*). Comparison of the harvested panicles of one plant individual in WT and the transgenic plants. (Scale bar, 5 cm.) (*D* and *E*) 1,000-grain weight *D* ($n = 10$) and yield per plant *E* ($n = 25$) of WT and the transgenic plants. Means ± SD were given, $^{*}P < 0.05$, $^{**}P < 0.01$ (*t* test). (*F* and *G*) Phenotypes of *BG1*-overexpressing plants in *Arabidopsis*. (Scale bar, 5 cm in *F* and 1 mm in *G*).

Although auxin was discovered more than 80 y ago and has been demonstrated to play important roles in many aspects of plant growth and development, in rice both auxin signaling and transport are poorly understood. Thus, identification of a novel auxin transport regulator in rice has great significance for understanding of auxin biology in monocotyledon. Although the mechanism for BG1 regulation of auxin transport remains elusive, this study establishes a connection between auxin transport and grain size, and demonstrates the feasibility of modulating auxin transport to enhance grain productivity, thus illuminating a new strategy to improve plant yield.

Materials and Methods

The *Bg1-D* mutant was identified from our T-DNA insertion population with *japonica* Nipponbare background (56). Details of experimental procedures, including plant cultivation, gene-expression analysis, histological analysis, RNA in situ hybridization, subcellular localization, IAA measurement, and auxin transport assay, are described in *SI Materials and Methods*. Primers used in this study are listed in Tables S3–S7.

ACKNOWLEDGMENTS. This work was supported by grants from National Natural Science Foundation of China (91335203), the Ministry of Agriculture of China (2014ZX08009-003-003, 2014ZX08001-004), and the Ministry of Science and Technology of China (2012CB944800).

1. Sakamoto T, Matsuoka M (2008) Identifying and exploiting grain yield genes in rice. *Curr Opin Plant Biol* 11(2):209–214.
2. Ikeda M, Miura K, Aya K, Kitano H, Matsuoka M (2013) Genes offering the potential for designing yield-related traits in rice. *Curr Opin Plant Biol* 16(2):213–220.
3. Xing Y, Zhang Q (2010) Genetic and molecular bases of rice yield. *Annu Rev Plant Biol* 61:421–442.
4. Song XJ, Huang W, Shi M, Zhu MZ, Lin HX (2007) A QTL for rice grain width and weight encodes a previously unknown RING-type E3 ubiquitin ligase. *Nat Genet* 39(5): 623–630.
5. Weng J, et al. (2008) Isolation and initial characterization of *GW5*, a major QTL associated with rice grain width and weight. *Cell Res* 18(12):1199–1209.
6. Shomura A, et al. (2008) Deletion in a gene associated with grain size increased yields during rice domestication. *Nat Genet* 40(8):1023–1028.
7. Ishimaru K, et al. (2013) Loss of function of the IAA-glucose hydrolase gene *TGW6* enhances rice grain weight and increases yield. *Nat Genet* 45(6):707–711.
8. Zhang X, et al. (2012) Rare allele of *OsPPKL1* associated with grain length causes extra-large grain and a significant yield increase in rice. *Proc Natl Acad Sci USA* 109(52):21534–21539.
9. Qi P, et al. (2012) The novel quantitative trait locus *GL3.1* controls rice grain size and yield by regulating Cyclin-T1;3. *Cell Res* 22(12):1666–1680.
10. Zuo J, Li J (2014) Molecular genetic dissection of quantitative trait loci regulating rice grain size. *Annu Rev Genet* 48(1):99–118.
11. Wang S, et al. (2012) Control of grain size, shape and quality by *OsSPL16* in rice. *Nat Genet* 44(8):950–954.
12. Miura K, Ashikari M, Matsuoka M (2011) The role of QTLs in the breeding of high-yielding rice. *Trends Plant Sci* 16(6):319–326.
13. Gonzalez N, Beemster GT, Inzé D (2009) David and Goliath: What can the tiny weed *Arabidopsis* teach us to improve biomass production in crops? *Curr Opin Plant Biol* 12(2):157–164.
14. Li J, Nie X, Tan JL, Berger F (2013) Integration of epigenetic and genetic controls of seed size by cytokinin in *Arabidopsis*. *Proc Natl Acad Sci USA* 110(38):15479–15484.
15. Schruff MC, et al. (2006) The *AUXIN RESPONSE FACTOR 2* gene of *Arabidopsis* links auxin signalling, cell division, and the size of seeds and other organs. *Development* 133(2):251–261.
16. Hu Y, Xie Q, Chua NH (2003) The *Arabidopsis* auxin-inducible gene *ARGOS* controls lateral organ size. *Plant Cell* 15(9):1951–1961.
17. Mizukami Y, Fischer RL (2000) Plant organ size control: *AINTEGUMENTA* regulates growth and cell numbers during organogenesis. *Proc Natl Acad Sci USA* 97(2): 942–947.
18. Teale WD, Paponov IA, Palme K (2006) Auxin in action: Signalling, transport and the control of plant growth and development. *Nat Rev Mol Cell Biol* 7(11):847–859.
19. Zhao Y (2010) Auxin biosynthesis and its role in plant development. *Annu Rev Plant Biol* 61:49–64.
20. Dai X, et al. (2013) The biochemical mechanism of auxin biosynthesis by an *Arabidopsis* YUCCA flavin-containing monooxygenase. *J Biol Chem* 288(3):1448–1457.
21. Zhao Y (2012) Auxin biosynthesis: A simple two-step pathway converts tryptophan to indole-3-acetic acid in plants. *Mol Plant* 5(2):334–338.
22. Wang B, et al. (2015) Tryptophan-independent auxin biosynthesis contributes to early embryogenesis in *Arabidopsis*. *Proc Natl Acad Sci USA* 112(15):4821–4826.
23. Chapman EJ, Estelle M (2009) Mechanism of auxin-regulated gene expression in plants. *Annu Rev Genet* 43:265–285.
24. Kepinski S, Leyser O (2005) The *Arabidopsis* F-box protein TIR1 is an auxin receptor. *Nature* 435(7041):446–451.
25. Dharmasiri N, Dharmasiri S, Estelle M (2005) The F-box protein TIR1 is an auxin receptor. *Nature* 435(7041):441–445.
26. Kim J, Harter K, Theologis A (1997) Protein-protein interactions among the Aux/IAA proteins. *Proc Natl Acad Sci USA* 94(22):11786–11791.
27. Bennett MJ, et al. (1996) *Arabidopsis AUX1* gene: A permease-like regulator of root gravitropism. *Science* 273(5277):948–950.
28. Gälweiler L, et al. (1998) Regulation of polar auxin transport by AtPIN1 in *Arabidopsis* vascular tissue. *Science* 282(5397):2226–2230.
29. Péret B, et al. (2012) AUX/LAX genes encode a family of auxin influx transporters that perform distinct functions during *Arabidopsis* development. *Plant Cell* 24(7): 2874–2885.
30. Balzan S, Johal GS, Carraro N (2014) The role of auxin transporters in monocots development. *Front Plant Sci* 5:393.
31. Reed RC, Brady SR, Muday GK (1998) Inhibition of auxin movement from the shoot into the root inhibits lateral root development in *Arabidopsis*. *Plant Physiol* 118(4): 1369–1378.
32. Noh B, Bandyopadhyay A, Peer WA, Spalding EP, Murphy AS (2003) Enhanced gravi- and phototropism in plant mdr mutants mislocalizing the auxin efflux protein PIN1. *Nature* 423(6943):999–1002.
33. Li P, et al. (2007) *LAZY1* controls rice shoot gravitropism through regulating polar auxin transport. *Cell Res* 17(5):402–410.
34. Okada K, Ueda J, Komaki MK, Bell CJ, Shimura Y (1991) Requirement of the auxin polar transport system in early stages of *Arabidopsis* floral bud formation. *Plant Cell* 3(7):677–684.
35. Liu YG, Mitsukawa N, Oosumi T, Whittier RF (1995) Efficient isolation and mapping of *Arabidopsis thaliana* T-DNA insert junctions by thermal asymmetric interlaced PCR. *Plant J* 8(3):457–463.
36. Wang H, et al. (2011) Computation-assisted SiteFinding-PCR for isolating flanking sequence tags in rice. *Biotechniques* 51(6):421–423.
37. Ulmasov T, Murfett J, Hagen G, Guilfoyle TJ (1997) Aux/IAA proteins repress expression of reporter genes containing natural and highly active synthetic auxin response elements. *Plant Cell* 9(11):1963–1971.
38. Vieten A, et al. (2005) Functional redundancy of PIN proteins is accompanied by auxin-dependent cross-regulation of PIN expression. *Development* 132(20):4521–4531.
39. Jensen PJ, Hangarter RP, Estelle M (1998) Auxin transport is required for hypocotyl elongation in light-grown but not dark-grown *Arabidopsis*. *Plant Physiol* 116(2): 455–462.
40. Lin R, Wang H (2005) Two homologous ATP-binding cassette transporter proteins, AtMDR1 and AtPGP1, regulate *Arabidopsis* photomorphogenesis and root development by mediating polar auxin transport. *Plant Physiol* 138(2):949–964.
41. Chae K, et al. (2012) *Arabidopsis SMALL AUXIN UP RNA63* promotes hypocotyl and stamen filament elongation. *Plant J* 71(4):684–697.
42. Keuskamp DH, et al. (2011) Blue-light-mediated shade avoidance requires combined auxin and brassinosteroid action in *Arabidopsis* seedlings. *Plant J* 67(2):208–217.
43. Kant S, Bi YM, Zhu T, Rothstein SJ (2009) *SAUR39*, a small auxin-up RNA gene, acts as a negative regulator of auxin synthesis and transport in rice. *Plant Physiol* 151(2): 691–701.
44. Qi J, et al. (2008) Mutation of the rice *Narrow leaf1* gene, which encodes a novel protein, affects vein patterning and polar auxin transport. *Plant Physiol* 147(4): 1947–1959.
45. Takai T, et al. (2013) A natural variant of *NAL1*, selected in high-yield rice breeding programs, pleiotropically increases photosynthesis rate. *Sci Rep* 3:2149.
46. Fujita D, et al. (2013) *NAL1* allele from a rice landrace greatly increases yield in modern indica cultivars. *Proc Natl Acad Sci USA* 110(51):20431–20436.
47. Zhang GH, et al. (2014) *LSCHL4* from *Japonica* Cultivar, which is allelic to *NAL1*, increases yield of indica super rice 93-11. *Mol Plant* 7(8):1350–1364.
48. Vanneste S, Friml J (2009) Auxin: A trigger for change in plant development. *Cell* 136(6):1005–1016.
49. Petrásek J, Friml J (2009) Auxin transport routes in plant development. *Development* 136(16):2675–2688.
50. Nick P, Han MJ, An G (2009) Auxin stimulates its own transport by shaping actin filaments. *Plant Physiol* 151(1):155–167.
51. Benjamins R, Scheres B (2008) Auxin: The looping star in plant development. *Annu Rev Plant Biol* 59:443–465.
52. Geldner N, et al. (2003) The *Arabidopsis* GNOM ARF-GEF mediates endosomal recycling, auxin transport, and auxin-dependent plant growth. *Cell* 112(2):219–230.
53. Friml J, et al. (2004) A PINOID-dependent binary switch in apical-basal PIN polar targeting directs auxin efflux. *Science* 306(5697):862–865.
54. Gil P, et al. (2001) BIG: A calossin-like protein required for polar auxin transport in *Arabidopsis*. *Genes Dev* 15(15):1985–1997.
55. Xu M, Zhu L, Shou H, Wu P (2005) A *PIN1* family gene, *OsPIN1*, involved in auxin-dependent adventitious root emergence and tillering in rice. *Plant Cell Physiol* 46(10): 1674–1681.
56. Ma Y, et al. (2009) Molecular analysis of rice plants harboring a multi-functional T-DNA tagging system. *J Genet Genomics* 36(5):267–276.